

Anomalous low temperature magnetic properties in bulk magnetite

X H Liu^{1,2,3}  and Z P Zhou^{1,2}

¹ State Key Laboratory for Superlattices and Microstructures, Institute of Semiconductors, Chinese Academy of Sciences, Beijing 100083, People's Republic of China

² Center of Materials Science and Optoelectronics Engineering, University of Chinese Academy of Sciences, Beijing 100049, People's Republic of China

E-mail: xionghualiu@semi.ac.cn

Received 10 September 2019, revised 21 November 2019

Accepted for publication 19 December 2019

Published 13 January 2020



Abstract

We systematically investigated the magnetic properties of a single crystal bulk Fe_3O_4 at low temperatures. Below Verwey transition, the magnetization versus temperature curves under zero-field cooling present anomalous behaviors for [100], [101] and [001] directions, respectively. Furthermore, at Verwey temperature, a high sensitivity of relative magnetization change ($\Delta M/M$) to small magnetic field and, in particular, a reversal of $\Delta M/M$ at moderate magnetic field range for [001] direction is observed. Our work demonstrates a very important role of magnetic axis reorientation effect in low temperature magnetic properties of magnetite, which will stimulate further research on the intricate microscopic physics mechanisms in this classic material.

Keywords: magnetite, magnetization, critical temperature, critical field

(Some figures may appear in colour only in the online journal)

1. Introduction

Magnetite (Fe_3O_4) is one of the most fascinating transition metal oxide materials in solid state physics owing to its rather unique and interesting set of electrical and magnetic properties. The high Curie temperature [1] and theoretically predicted half-metallic behavior [2] make magnetite a promising candidate for applications in various spintronics devices [3–6]. Besides the two orders jump in resistivity at Verwey temperature (T_V) [7], the Fe_3O_4 is known to exhibit the reduction in magnetization with cooling temperature across T_V , and the magnitude of the discontinuity magnetization ΔM depends on the external magnetic field and the orientation of the Fe_3O_4 [8–26]. The variation of relative magnetization $\Delta M/M$ reduces with increasing magnetic field [8, 9, 14], and reaches about 0.1% under saturated magnetic field [10, 11, 14], where ΔM is the difference between the magnetization at temperature just above and below T_V , and M is the magnetization just above T_V . However, it is worth noting that all the previous works only exhibit the positive ΔM , that the magnetization at

temperature just above T_V is always larger than that below T_V [8–26]. Furthermore, as the oldest magnetic material known to mankind, the magnetic properties of magnetite have been widely studied in past several centuries, whereas the mechanism of some magnetic properties below Verwey transition is still not clear [8–14, 27].

In this work, we systematically studied the magnetic properties of a single-crystal bulk Fe_3O_4 at low temperatures measured along [100], [101] and [001] directions. Below T_V , the zero-field-cooled (ZFC) $M(T)$ curves exhibit different field-dependence of critical temperatures behaviors. Furthermore, at T_V we found a great sensitivity of $\Delta M/M$ to small magnetic field and, remarkably, an unusual reversal of ΔM at moderate magnetic field range for [001] direction. Our work suggests that the low temperature magnetic properties of bulk magnetite are significantly related to the magnetic axis orientations.

2. Experimental

The Fe_3O_4 single crystal was grown by floating zone technique [18]. The high quality of our Fe_3O_4 single crystal can be confirmed by powder and single crystal x-ray diffraction

³ Author to whom any correspondence should be addressed.

at room temperature, as well as temperature dependent magnetic and transport properties measurements [27]. A high $T_V \sim 124$ K with more than two orders jump in resistivity and a narrow hysteresis of 0.3 K indicates the high sample quality [see inset of figure 1(a)] [28–30]. The single crystal bulk was cut into a bar-shaped cuboid with dimensions of 6.5 mm [100] \times 2.2 mm [010] \times 1.0 mm [001]. Throughout this article, crystal axes of [100], [101], and [001] refer to the high temperature cubic structure. The transport and magnetic properties measurements of the single crystal bulk were carried out by standard four probe technique using a physical property measurement system (PPMS) and superconducting quantum interference device (SQUID), respectively. The temperature dependence of resistivity $\rho(T)$ curve was performed at zero field with current source 1 μ A from 300 K to 50 K and back to 300 K. The zero-field-cooled and field-cooled (ZFC-FC) $M(T)$ curves were measured with field along [100], [101] and [001] respectively, under different external magnetic fields with scanning temperature from 10 K to 300 K and back to 10 K. For the initial $M(H)$ measurements, the system is ZFC from 300 K to aim temperature and then applied magnetic field from 0 to 50 kOe.

3. Results and discussion

It has been reported that bulk Fe_3O_4 exhibits complicated physical properties at low temperatures. Apart from the well-known $T_V = 124$ K and a magnetocrystalline anisotropy isotropic point $T_K = 130$ K [14], Fe_3O_4 is also reported to show an anomaly increase in susceptibility around 30 to 50 K [12], a ferroelectric transition at about 38 K [31], and an reversal of magnetoresistance at around 78 K [27]. Figure 1(a) shows the ZFC-FC $M(T)$ curve along [100] direction under 30 kOe, besides a small jump in magnetization at T_V , another abrupt increase in magnetization for ZFC branch takes place at 47 K (marked as T_{sw1}), which is not reported in bulk Fe_3O_4 yet [8–14]. The T_{sw1} gradually shifts to high temperature with decreasing magnetic field [see figures 1(a)–(c)]. Similar phenomenon is also observed along [001] direction in figures 1(d)–(f).

A normal change in magnetization (positive ΔM) at T_V under different magnetic fields was observed in figures 1(a)–(c) [8–17, 19–26]. At high magnetic field ($H \geq 5$ kOe), the $\Delta M/M$ is close to 0.1% [11, 13], which increases with reducing magnetic field (figure 1(c)). Figure 1(d) also presents the normal magnetization change $\Delta M/M$ of about 0.1%. However, the $M(T)$ curve under 5 kOe displays a reversal of ΔM at T_V in figure 1(e). With decreasing magnetic field further, the ΔM returns to its normal sign (positive) again (figure 1(f)). Obviously, the reversal of magnetization at T_V only happens at moderate magnetic field range.

The $\Delta M/M$ versus H at T_V for [100] and [001] directions are plotted in figures 2(a) and (c), respectively. Figure 2(a) shows a typical variation of $\Delta M/M$ with magnetic field in bulk Fe_3O_4 [8–14], the $\Delta M/M$ sharply decreases with increasing field from 0.1 to 1 kOe and becomes nearly constant of about 0.1% over 5 kOe. For comparison, the change of $\Delta M/M$

with H at small fields is slower along [001] [figure 2(c)]. Especially, the $\Delta M/M$ changes sign at $H > 3.7$ kOe and gets to a minimum of -1.37% for 4 kOe. With further increasing field, the $\Delta M/M$ gradually increases and reverses to positive again at 10 kOe, and then it keeps nearly constant of 0.1% at $H > 10$ kOe.

More interesting phenomena were found for the bulk Fe_3O_4 measured along [101] direction in figure 3. Under high magnetic field [figure 3(a)], the ZFC branch exhibits a new rapid drop in magnetization (marked as T_{sw2}), instead of a sharp increase in magnetization at T_{sw1} in figure 1. The value of T_{sw2} gradually moves to low temperature with reducing magnetic field [see figures 3(a)–(c)]. Remarkably, both T_{sw1} and T_{sw2} , which forms a platform, appears for 10 kOe in figure 3(c). This platform gradually shrinks with lowering magnetic field and disappears for 3 kOe [see figure 3(e)].

The magnetic fields corresponding to T_{sw1} and T_{sw2} , respectively, as a function of temperature is summarized as an inset of figure 3(a). The T_{sw1} and T_{sw2} as a function of external magnetic fields is summarized as an inset of figure 3(a). The T_{sw1} can be found from 33 to 120 K at $H \leq 10$ kOe, while the T_{sw2} can be noticed only from 61 to 85 K at fields between 5 and 40 kOe. In particular, the magnetization for ZFC branch is larger than that of the FC branch below T_{sw2} [see figures 3(a)–(c)], which is contrast to the results in figure 1 and also never reported in previous work [8–17, 19–26]. Importantly, these anomalous magnetic behaviors were only observed in ZFC branch. Compared to the small $\Delta M/M$ under moderate magnetic fields at T_V in figure 2(a), the values for [101] direction are much larger [figure 2(b)], the $\Delta M/M$ gradually decreases from 10% at 0.7 kOe to 0.65% at 30 kOe.

The abrupt jump in magnetization at T_{sw1} and the increase of T_{sw1} with reducing magnetic field, observed only in ZFC branch in figures 1 and 3, reminds us to consider the magnetic easy axis reorientation effect for the bulk transformed from cubic $Fd\bar{3}m$ to monoclinic Cc structure [27, 32]. It has been reported that the easy magnetization axis (hard magnetization axis) varies from [111] ([100]) above T_K to [100] ([111]) for temperatures below T_K [9, 32, 33]. Under ZFC condition, small magnetic domains of different orientations of the easy magnetization axis in the monoclinic phase are formed. In this case the initial magnetization state below T_V can be considered as almost identical because the sample is nearly completely demagnetized by zero field cooling from 300 K (well above T_K) [34]. The initial magnetization processes upon application of the external field then aligns these magnetic domains for fields higher than a critical one. Correspondingly, the initial $M(H)$ curve after zero field cooling from high temperature to below T_V exhibits a sharp jump in magnetization at a critical field (H_{cr}), here H_{cr} is defined as the maximum slope of $M(H)$ curve [27]. Figures 4(a) and (b) show the initial $M(H)$ curves at different temperatures after zero field cooling from 300 K measured along [100] and [101] directions, respectively. A sharp jump in magnetization can be observed at H_{cr} , which gradually enhances with lowering temperature and nearly disappears at 45 K in figures 4(a) and (b). The H_{cr} from $M(H)$ curves at different temperatures in figures 4(a) and (b) and the

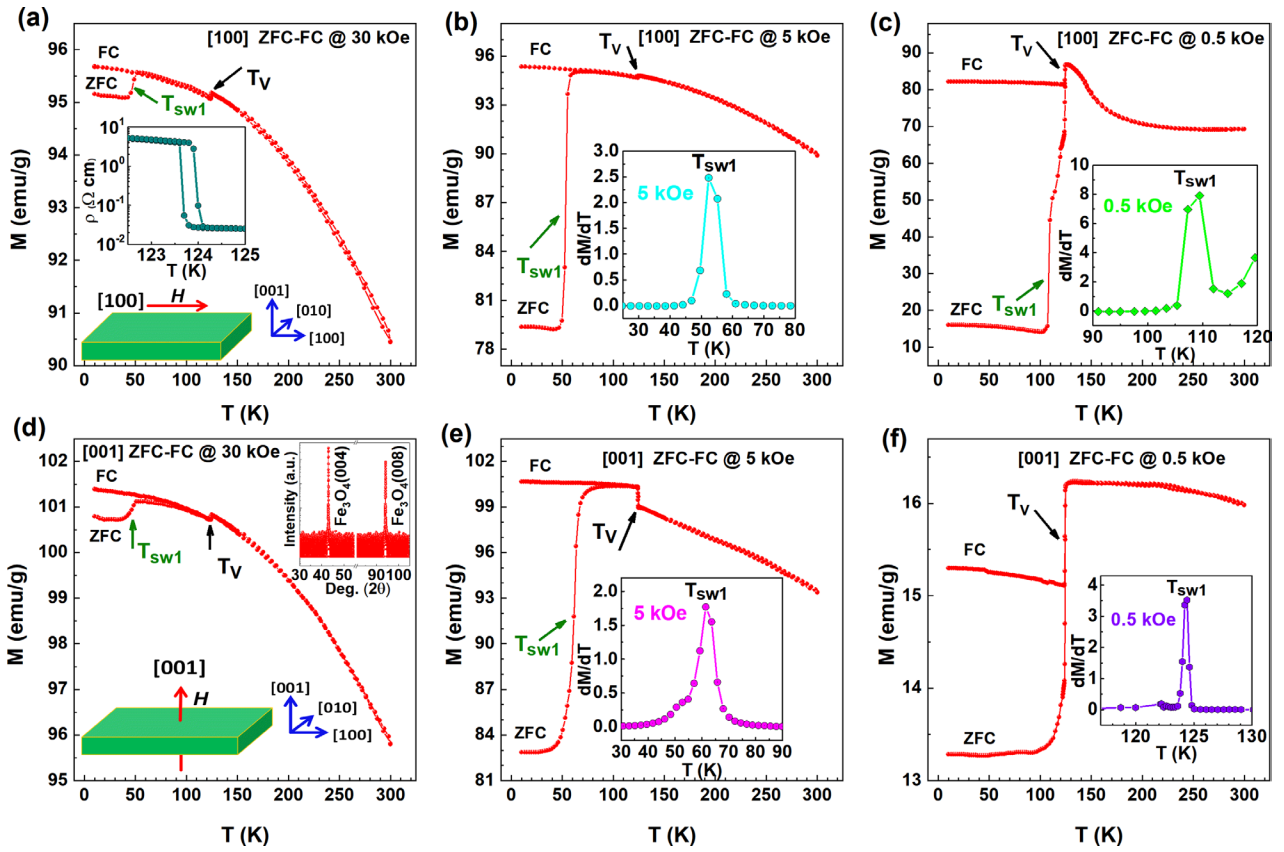


Figure 1. (a) ZFC-FC curve of bulk Fe_3O_4 at 30 kOe with temperature from 10 to 300 K for [100] direction. Inset: (up) Resistivity as a function of temperature in the vicinity of Verwey transition at zero field; (down) Schematic picture of the measurement setup along the crystallographic [100] direction. (b) and (c) ZFC-FC curves at 5 and 0.5 kOe along [100] direction, respectively. The insets show dM/dT versus T in the vicinity of $T_{\text{sw}1}$. (d)–(f) ZFC-FC curves at 30, 5 and 0.5 kOe along [001] direction, respectively. The insets of (d)–(f) present schematic picture of the measurement setup and the single crystal x-ray diffraction result for Fe_3O_4 bulk, dM/dT versus T around $T_{\text{sw}1}$ at 5 and 0.5 kOe, respectively.

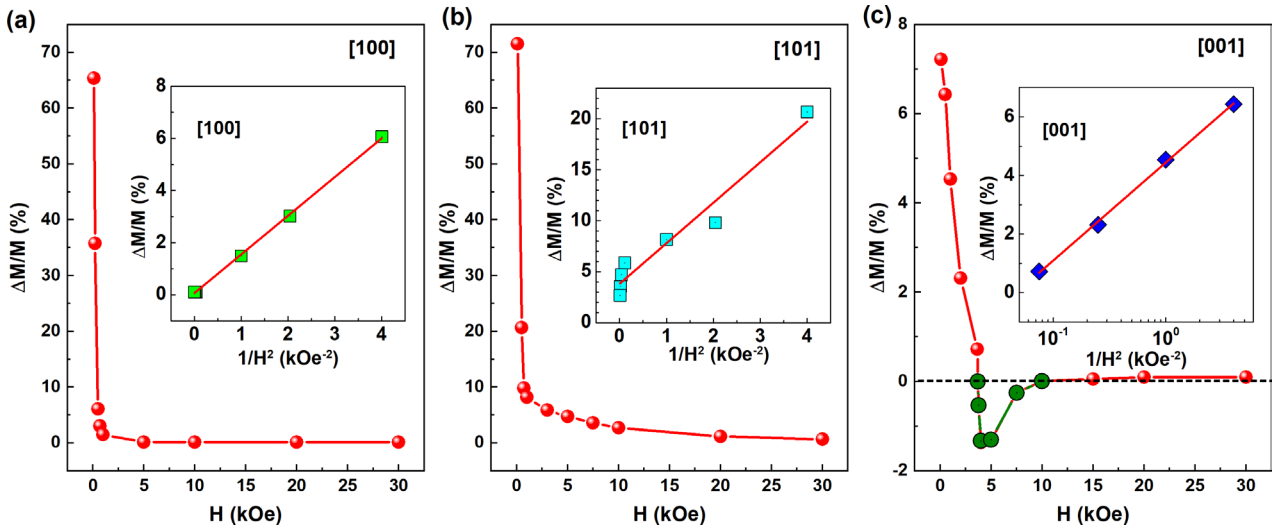


Figure 2. (a)–(c) Magnetic field dependence of $\Delta M/M$ at T_V along [100], [101] and [001] directions, respectively. The insets show the $\Delta M/M$ versus $1/H^2$ for three directions. It can be seen that the $\Delta M/M$ linearly changes with $1/H^2$ for [100] and [101] while with $\log(1/H^2)$ for [001] direction. The linear slope of $\Delta M/M$ versus $1/H^2$ for [101] is about three times larger than that for [100].

$H_{\text{sw}1}$ corresponding to $T_{\text{sw}1}$ from ZFC curves in figures 1 and 3 along [100] and [101] directions, are plotted in figures 4(c) and (d), respectively. The nice coincident results demonstrate that the abrupt jump in magnetization at $T_{\text{sw}1}$ is indeed caused

by the magnetic axis reorientation in the bulk [27]. For the FC condition, the magnetic domains are aligned during the field cooling, that a single-crystalline structure can be retained by simultaneously applying an external magnetic field upon

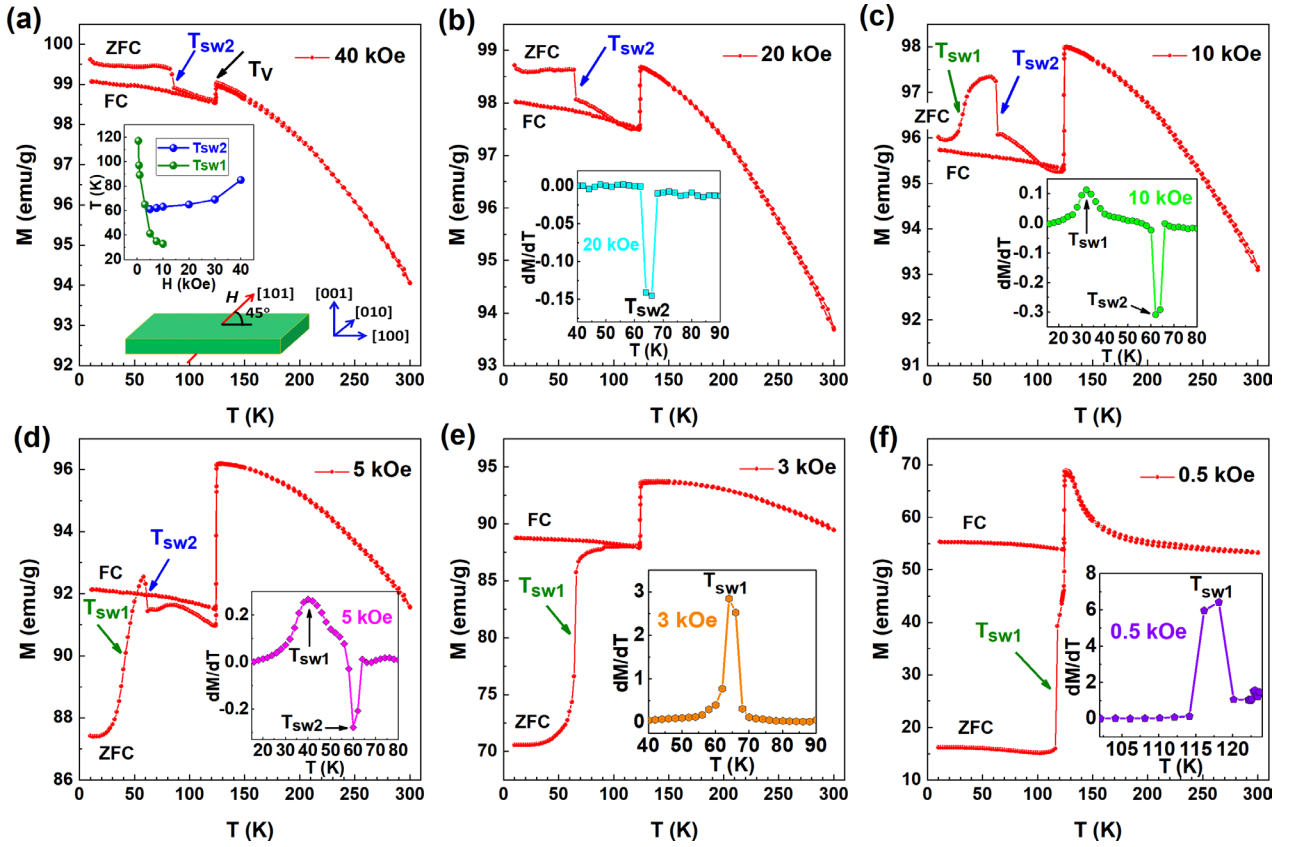


Figure 3. (a)–(f) ZFC-FC curves at 40, 20, 10, 5, 3 and 0.5 kOe, respectively, for [101] direction. The schematic picture of the measurement setup along [101] and the T_{sw1} and T_{sw2} as a function of external magnetic fields are shown as an inset of (a). The insets of (b)–(f) display dM/dT versus T with positive and negative extremum for T_{sw1} and T_{sw2} , respectively.

cooling through T_V (which aligns the easy magnetization axis, i.e. the crystallographic c^* -axes that are perpendicular to the monoclinic a - b planes) as well as mechanically straining the sample in order to de-twin the Fe_3O_4 single crystal [35]. Thus the larger magnetization for FC branch than that for ZFC branch below T_V is observed in figure 1.

It has been reported that the variation in magnetization is significantly related to external magnetic field and the orientation of bulk Fe_3O_4 at T_V (see figures 1–3). Umemura. *et al*, investigated the angular dependence of $\Delta M/M$ under saturated magnetic field at T_V and proposed that the decrease in magnetization is related to the magnetic anisotropy energy of bulk Fe_3O_4 [10]. The magnitude of the discontinuity value can be expressed as

$$\Delta M/M = [1/(2M_S^2 H^2)] (|\text{grad}E_{an}|^2 - |\text{grad}E'_{an}|^2), \quad (1)$$

where M_S is the spontaneous magnetization, E_{an} and E'_{an} are the magnetic anisotropy energies at just below and above the T_V , respectively. As the E_{an} of monoclinic structure is extremely larger than E'_{an} of cubic structure [10, 14], in sufficiently strong fields, $|\text{grad}E'_{an}|^2$ can be neglected, thus

$$\Delta M/M = [1/(2M_S^2 H^2)] (|\text{grad}E_{an}|^2). \quad (2)$$

That the $\Delta M/M$ is proportional to $1/H^2$, which is nicely shown in the inset of figure 2(a) for [100] while is not well fitted for

[101] direction [see inset of figure 2(b)]. However, the $\Delta M/M$ for [001] direction exhibits linear increase with $\log(1/H^2)$ [see inset of figure 2(c)]. In particular, the negative $\Delta M/M$ cannot be obtained from the equation (2).

Recently, the Verwey transition is considered to be determined by interplay among charge, orbital and lattice degrees of freedom. Although the driving force, that the charge-orbital ordering or electron–phonon coupling being responsible for this transition, is still debated [36–44], yet, the on-site Coulomb interaction between 3d electrons for iron ions and the lattice distortion from cubic to monoclinic are considered to be indispensable ingredients for the Verwey transition. Whereas, this anomalous negative $\Delta M/M$ at T_V cannot be well explained by this structural-electronic model. Furthermore, Belov proposed a magneto–electronic model to interpret the Verwey transition in Fe_3O_4 [14, 45, 46], in which an e-sublattice is formed due to the existence of Vonsovskii exchange interaction. As the Vonsovskii exchange interaction between the hopping electrons and the inner electrons of iron cations is negative (antiferromagnetic), which leads not only to localization of the conduction electrons but also to a partial screening of the total magnetic moment, corresponding to the decrease in magnetization on cooling through T_V (positive ΔM). With increasing external field, the e-sublattice gradually weakens, resulting in the gradual decrease in $\Delta M/M$, similar to that shown in figures 1(a)–(c), 2(a), (b) and 3. This model, however, also could not give out a reversal of $\Delta M/M$ at T_V

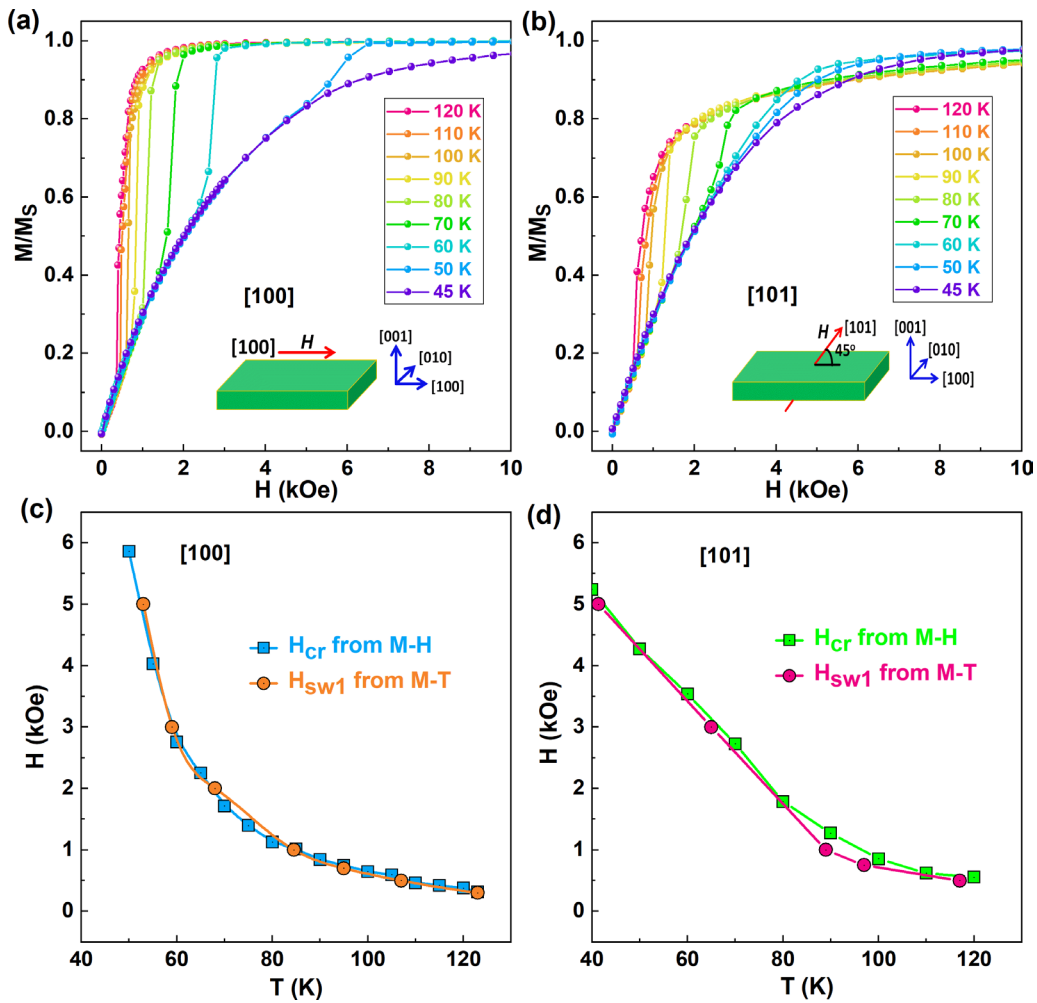


Figure 4. (a) and (b) Initially normalized magnetization (M/M_s) as a function of magnetic field at different temperatures after ZFC from 300 K for [100] and [101], respectively. (c) and (d) Temperature dependence of critical field H_{sw1} , corresponding to the field at T_{sw1} , obtained from ZFC curves and (H_{cr}) from $M(H)$ curves after ZFC from 300 K for [100] and [101], respectively.

shown in figures 1(e) and 2(c). Thus our work in fact gives a new example in this issue, which not only help us deeply understand the Verwey transition but also in turn provides a tool to testify different models.

Furthermore, the sharp drop in magnetization at T_{sw2} and larger magnetization for ZFC branch in figure 3 make us to think the compensation behavior in some multiferroic spinel oxides in which the magnetization of ZFC is larger than that of FC when applied magnetic field is smaller than coercivity field below the compensation temperature [47–49]. For these ferrimagnetic spinel oxides, the spin moments of tetrahedral (A) sites are antiparallel to octahedral (B) sites, the temperature dependence of magnetic moments and the competition between antiferromagnetic interaction in A/B sites and ferromagnetic interaction between ions in B sites lead to the compensation effect. It has been reported that the exchange integral values are $J_{AB} = -22$ K, $J_{BB} = 3$ K, and $J_{AA} = -11$ K in bulk Fe_3O_4 [50], the J_{AB} dominates the interactions. Moreover, the compensation behavior in multiferroic spinel oxides usually occurs at small magnetic field [47–49], whereas the abrupt reduction in magnetization at T_{sw2} combined with the larger magnetization of ZFC branch only take place under high fields

[see figures 3(a)–(c)]. Thus the magnetic properties about T_{sw2} would be not related to the compensation behavior [47–49].

In addition, Zhang *et al* theoretically gave some interesting phenomena in two sub-lattice system using mean-field model [51]. The sharp jump of magnetization, corresponding to the first-order spin reorientation transitions in $M(T)$ curve, is based on the competition among the exchange and the anisotropies of the two sublattices. The canting spin instead of completely parallel or antiparallel structures might happen in some special conditions [51]. It is known that the [100] or [001] is the equal easy axis below T_V [9, 32, 33] though the shape anisotropy is much smaller for the former in our system. When measuring ZFC-FC curves with applied field along these two directions, the spin moments of A and B are always antiparallel, corresponding to the smaller magnetization of ZFC than that of FC branch at $T < T_V$.

However, for the measurement along [101] direction, a small angle between A and B sites may exist under strong magnetic field. Especially, all these anomalous behaviors, only observed for ZFC condition, suggest that the magnetic axis reorientation effect involves in this complex interactions. At low temperature, the magnetic axis reorientation effect,

to some extent, can assist Zeeman interaction overcome the strong antiferromagnetic interaction between A and B sites to keep the system in a metastable state (a small angle between A and B sites).

The gradual reduction of easy axis reorientation effect with rising temperature (see the drop of H_{cr} in figure 4) or the decrease of Zeeman interaction (smaller external magnetic field) will result in the breakdown of this metastable state, corresponding to the sharp drop in magnetization at T_{sw2} . Then the system returns to its normal state with antiparallel of A and B sites, like the first-order spin reorientation transition from canting one to completely antiparallel coupling [51]. Thus a clear reduction of T_{sw2} with decreasing external magnetic field is observed [see inset of figure 3(a)].

When field-cooling system from high temperature, the magnetic axis reorientation effect disappears [27], while the Zeeman interaction is not strong enough to compete with antiferromagnetic coupling between A and B sites. Thus the spin moments of A and B sites are always antiparallel, the smaller magnetization for FC than that for ZFC branch is observed below T_{sw2} . Moreover, it is observed from figures 3(a)–(c) that the relative variation of magnetization between ZFC and FC is about 1%, meaning the canting angle between A and B sites is about 6°.

4. Conclusion

We have systematically investigated the magnetic properties of a single crystal bulk Fe_3O_4 at low temperatures. Below T_V , the ZFC curves show different kinds of field dependence of critical temperatures (T_{sw1} or T_{sw2}) for [100], [101] and [001] directions, respectively. Furthermore, at T_V we observed a high sensitivity of $\Delta M/M$ to small magnetic field and, in particular, an unusual reversal of $\Delta M/M$ at some magnetic field range for [001] direction. Our work demonstrates a very important role of magnetic axis reorientation effect in low temperature magnetic properties of magnetite.

Acknowledgments

This work was supported by the National Key R&D Program of China No. 2017YFB0405700. This work was also supported by the NSFC Grant Nos. 11474272 and 61774144. The Project was sponsored by the Chinese Academy of Sciences, Grant Nos. QYZDY-SSW-JSC020, XDB28000000, and XDPB12.

ORCID iDs

X H Liu  <https://orcid.org/0000-0003-1237-2787>

References

- [1] Garcia J and Subias G 2004 *J. Phys.: Condens. Matter* **16** R145
- [2] de Groot R A, Mueller F M, van Engen P G and Buschow K H J 1983 *Phys. Rev. Lett.* **50** 2024
- [3] Li X W, Gupta A, Xiao G, Qian W and Dravid V P 1998 *Appl. Phys. Lett.* **73** 3282
- [4] Hu G and Suzuki Y 2002 *Phys. Rev. Lett.* **89** 276601
- [5] Liu X H, Rata A D, Chang C F, Komarek A C and Tjeng L H 2014 *Phys. Rev. B* **90** 125142
- [6] Imada M, Fujimori A and Tokura Y 1998 *Rev. Mod. Phys.* **70** 1039
- [7] Verwey E J W 1939 *Nature* **144** 327
- [8] Domenicali C A 1950 *Phys. Rev.* **78** 458
- [9] Calhoun B A 1954 *Phys. Rev.* **94** 1577
- [10] Umemura S and Iida S 1976 *J. Phys. Soc. Japan* **40** 679
- [11] Aragón R 1992 *Phys. Rev. B* **46** 5328
- [12] Moskowitz B M, Jackson M and Kissel C 1998 *Earth Planet. Sci. Lett.* **157** 141
- [13] Özdemir Ö and Nunlop D J 1999 *Earth Planet. Sci. Lett.* **165** 229
- [14] Muxworthy A R and McClelland E 2000 *Geophys. J. Int.* **140** 101
- [15] Gong G Q, Gupta A, Xiao G, Qian W and Dravid V P 1997 *Phys. Rev. B* **56** 5096
- [16] Ogale S B, Ghosh K, Sharma R P, Greene R L, Ramesh R and Venkatesan T 1998 *Phys. Rev. B* **57** 7823
- [17] Ziese M and Blythe H J 2000 *J. Phys.: Condens. Matter* **12** 13
- [18] Delille F, Dieny B, Moussy J B, Guittet M J, Gota S, Gautier-Soyer M and Marin C 2005 *J. Magn. Magn. Mater.* **294** 27
- [19] Arora S K, Wu H C, Choudhary R J, Shvets I V, Mryasov O N, Yao H and Ching W Y 2008 *Phys. Rev. B* **77** 134443
- [20] Liu X H, Liu W and Zhang Z D 2017 *RSC Adv.* **7** 43648
- [21] Orna J *et al* 2010 *Phys. Rev. B* **81** 144420
- [22] Liu X H, Liu W and Zhang Z D 2017 *Phys. Rev. B* **96** 094405
- [23] Alraddadi S, Hines W, Yilmaz T, Gu G D and Sinkovic B 2015 *J. Phys.: Condens. Matter* **28** 115402
- [24] Liu X, Mi W B, Zhang Q and Zhang X X 2017 *Phys. Rev. B* **96** 214434
- [25] Liu X, Mi W B, Zhang Q and Zhang X X 2018 *Appl. Phys. Lett.* **113** 012401
- [26] Liu X H, Liu W, Zhang Z D and Chang C F 2018 *J. Appl. Phys.* **123** 083903
- [27] Liu X H, Chang C F, Tjeng L H, Komarek A C and Wirth S 2019 *J. Phys.: Condens. Matter* **31** 225803
- [28] Aragon R, Buttrey D J, Shepherd J P and Honig J M 1985 *Phys. Rev. B* **31** 430
- [29] Kakol Z, Sabol J, Stickler J and Honig J M 1992 *Phys. Rev. B* **46** 1975
- [30] Honig J M 1995 *J. Alloys Compd.* **229** 24
- [31] Alexe M, Ziese M, Hesse D, Esquinazi P, Yamauchi K, Fukushima T, Picozzi S and Gösele U 2009 *Adv. Mater.* **21** 4452
- [32] Kakol Z *et al* 2011 *J. Phys.: Conf. Ser.* **303** 012106
- [33] Wright J P, Attfield J P and Radaelli P G 2002 *Phys. Rev. B* **66** 214422
- [34] Özdemir Ö 2000 *Geophys. J. Int.* **141** 351
- [35] Iizumi M, Koetzle T F, Shirane G, Chikazumi S, Matsui M and Todo S 1982 *Acta Cryst. B* **38** 2121
- [36] Wright J P, Attfield J P and Radaelli P G 2001 *Phys. Rev. Lett.* **87** 266401
- [37] Subias G, Garcia J, Blasco J, Proietti M G, Renevier H and Sanchez M C 2004 *Phys. Rev. Lett.* **93** 156408
- [38] Leonov I, Yaresko A N, Antonov V N, Korotin M A and Anisimov V I 2004 *Phys. Rev. Lett.* **93** 146404
- [39] Rozenberg G Kh, Pasternak M P, Xu W M, Amiel Y, Hanfland M, Amboage M, Taylor R D and Jeanloz R 2006 *Phys. Rev. Lett.* **96** 045705
- [40] Piekarczyk P, Parlinski K and Oles A M 2006 *Phys. Rev. Lett.* **97** 156402

- [41] Lorenzo J E, Mazzoli C, Jaouen N, Detlefs C, Mannix D, Grenier S, Joly Y and Marin C 2008 *Phys. Rev. Lett.* **101** 226401
- [42] Senn M S, Wright J P and Attfield J P 2012 *Nature* **481** 173
- [43] Liu X H, Chang C F, Rata A D, Komarek A C and Tjeng L H 2016 *npj Quantum Mater.* **1** 16027
- [44] Liu X H, Liu W, Dai Z M, Li S K, Wang T T, Cui W B, Li D, Komarek A C, Chang C F and Zhang Z D 2017 *Appl. Phys. Lett.* **111** 212401
- [45] Belov K P 1993 *Phys.-Usp.* **36** 380
- [46] Belov K P 1994 *Phys.-Usp.* **37** 563
- [47] Padam R, Pandya S, Ravi S, Nigam A K, Ramakrishnan S, Grover A K and Pal D 2013 *Appl. Phys. Lett.* **102** 112412
- [48] Zhang H G, Wang W H, Liu E K, Tang X D, Li G J, Zhang H W and Wu G H 2013 *Phys. Status Solidi b* **7** 1287
- [49] Zhang H G, Wang Z, Liu E K, Wang W H, Yue M and Wu G H 2015 *J. Appl. Phys.* **117** 17B735
- [50] De Grave E, Persoons R M, Vandenberghe R E and de Bakker P M A 1993 *Phys. Rev. B* **47** 5881
- [51] Zhang Z D, Yu M H and Zhao T 1997 *J. Magn. Magn. Mater.* **174** 261